

Surface Catalytic Mechanism in Square-Wave Voltammetry

Valentin Mirčeski* and Rubin Gulaboski

Institute of Chemistry, Faculty of Natural Sciences and Mathematics, "Sv. Kiril i Metodij" University, P.O. Box 162, 91001 Skopje, Republic of Macedonia; e-mail: valentin@iunona.pmf.ukim.edu.mk

Received: November 17, 2000

Final version: March 1, 2001

Abstract

A pseudo-first-order catalytic mechanism in which both reactant and product of the redox reaction are strongly immobilized on the electrode surface is theoretically analyzed under conditions of square-wave voltammetry (SWV). A mathematical procedure is developed for diffusionless conditions. The relationships between the properties of the voltammetric response and both the kinetic parameters of the redox reaction and the parameters of the excitement signal are studied. The phenomenon of the quasireversible maximum is discussed. The theoretical results are confirmed with the experiments of azobenzene performed in a presence of hydrogen peroxide. In acetate buffer with pH 4.2 the standard rate constant of charge transfer of azobenzene is $k_s = 12 \text{ s}^{-1}$ and the catalytic rate constant in the presence of hydrogen peroxide is $k_c = 2.24 \times 10^4 \text{ s}^{-1} \text{ mol}^{-1} \text{ L}$.

Keywords: Surface catalytic mechanism, Square-wave voltammetry, Azobenzene, Hydrogen peroxide

1. Introduction

Sensitivity of a particular voltammetric method can be significantly enhanced if one or both species of the redox couple exhibits a tendency for adsorption to the working electrode surface. A similar effect on the sensitivity of the method can be achieved if the product of the redox reaction regenerates the substance reacting at the electrode, by means of a homogenous chemical reaction. The latter case, known as a catalytic electrode mechanism, attracted considerable interest in the theory of classical DC polarography [1–4], double potential step chronoamperometry [5], differential pulse polarography [6], and square-wave voltammetry [7, 8].

Obviously, an electrode mechanism in which both adsorption and catalytic phenomena simultaneously occur, is of certain analytical importance, because both phenomena can contribute to the sensitivity of a voltammetric method. In this article a catalytic electrode mechanism in which both reactant and product of the redox couple are strongly adsorbed on the electrode surface is theoretically treated under conditions of square-wave voltammetry (SWV). Such an electrode mechanism has not been considered in the theory of the SWV so far. The study of this electrode mechanism with SWV is of considerable importance since this technique appears to be one of the most advanced and most sensitive electroanalytical techniques. Moreover, recently it was demonstrated that this technique is especially convenient for both kinetic characterization [9–15] and quantitative determination [16] of the redox couples strongly immobilized on the electrode surface. The theoretical results presented in this article are verified by the experiments performed with the well-known redox couple azobenzene/hydrazobenzene, in the presence of hydrogen peroxide, as a catalytic reagent.

2. Theoretical Model

A pseudo-first-order surface catalytic mechanism, in which both species of the redox couple are strongly immobilized on the electrode surface, is considered:



It is assumed that the reaction is controlled by the charge transfer kinetics as well as by the kinetics of the pseudo-first-order "catalytic" Reaction II. In addition, it is assumed that the adsorption of both reactant and product of the redox reaction is totally irreversible, that there is no significant interactions between the adsorbed molecules in the case of submonolayer surface coverage and that the additional adsorption in the course of the voltammetric measurements and the redox reaction of the dissolved molecules, can be neglected. Under these conditions, the above electrode mechanism is described by the following differential equations:

$$I/(nFS) = -d\Gamma_{\text{Ox}}/dt + k_c\Gamma_{\text{Red}} \quad (1)$$

$$I/(nFS) = d\Gamma_{\text{Red}}/dt + k_c\Gamma_{\text{Red}} \quad (2)$$

which are solved at the following boundary conditions:

$$t = 0: \quad \Gamma_{\text{Ox}} = \Gamma_0, \quad \Gamma_{\text{Red}} = 0,$$

$$t > 0: \quad \Gamma_{\text{Ox}} + \Gamma_{\text{Red}} = \Gamma_0$$

where Γ_{Ox} and Γ_{Red} are surface concentrations of Ox and Red species, respectively, while Γ_0 is the initial concentration of the Ox specie. k_c is a pseudo-first-order "catalytic" rate constant of the Reaction II expressed in s^{-1} . It is defined as $k_c = k'_c c(\text{Cat})$ where k'_c is a real rate constant of the "catalytic" reaction in $\text{s}^{-1} \text{ mol}^{-1} \text{ L}$, while $c(\text{Cat})$ is the concentration of the oxidizing agent Cat, present in large excess.

The solutions of the Equations 1 and 2 were obtained applying Laplace transformations. The solutions reads:

$$\Gamma_{\text{Ox}} = \Gamma_0 - \int_0^t \frac{I(\tau)}{nFS} e^{-k_c(t-\tau)} d\tau \quad (3)$$

and

$$\Gamma_{\text{Red}} = \int_0^t \frac{I(\tau)}{nFS} e^{-k_c(t-\tau)} d\tau \quad (4)$$

Equations 3 and 4 represent the relationship between current and time, during a certain constant potential.

If the redox reaction (I) is controlled by charge transfer kinetics, the following condition is valid at the electrode surface:

$$I/(nFS) = k_s \exp(-\alpha\phi) [\Gamma_{\text{Ox}} - \exp(\phi) \Gamma_{\text{Red}}] \quad (5)$$

Here, k_s is standard rate constant of the redox reaction (I) expressed in unit s^{-1} , α is transfer coefficient, ϕ is relative dimensionless electrode potential defined as $\phi = nF(E - E^0)/(RT)$. All other symbols have their usual meanings. Substituting Equations 3 and 4 in Equation 5, the integral equation which represents the solution for a quasi-reversible redox reaction is obtained:

$$\frac{I}{nFS} = k_s e^{-\alpha\phi} \Gamma_0 - k_s e^{-\alpha\phi} (1 + e^{\phi}) \int_0^t \frac{I(\tau)}{nFS} e^{-k_c(t-\tau)} d\tau \quad (6)$$

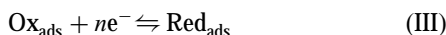
The numerical solutions of the latest integral Equation 6 was obtained by the method of Nicholson and Olmstead [17]. The numerical solution reads:

$$\Psi_m = \frac{\lambda e^{-\alpha\phi_m} \left(1 - \frac{1 + e^{\phi_m}}{\gamma} \sum_{j=1}^{m-1} \Psi_j M_{m-j+1} \right)}{1 + \lambda e^{-\alpha\phi_m} (1 + e^{\phi_m}) \frac{M_1}{\gamma}} \quad (7)$$

where Ψ is the dimensionless current defined as $\Psi = I/(nFS\Gamma_0f)$, $\gamma = k_c/f$ is the dimensionless catalytic parameter, $\lambda = k_s/f$ is the dimensionless kinetic parameter and f is the frequency of the signal. The numerical integration factor M is defined as:

$$M_k = e^{-(\gamma/50)(k-1)} - e^{-(\gamma/50)k}$$

If $\gamma \rightarrow 0$, the solution (Eq. 7) is equal with the corresponding solution for a simple surface redox reaction, which is well known in the literature [11, 12, 15]:



This fact proves that the above mathematical model is correctly solved. The solution of the redox reaction III is used for a comparison with the surface catalytic electrode mechanism.

3. Experimental

All chemicals used were of analytical reagent grade ("Merck" products). Redistilled water was used. 0.1 mol/L acetate buffer solutions were used as supporting electrolytes. A stock solution of hydrogen peroxide with concentration of 8% (w/w) was used. The amounts of hydrogen peroxide that were added in the electrolyzed solutions are indicated in the caption of the figures. The volume of the electrolyzed solution was 10 mL. The stock solution of azobenzene was prepared by dissolving in glacial acetic acid. Extra pure nitrogen was used for purging the electrolyte solutions for ten minutes prior to each measurement. A nitrogen blanket, over the electrolyte solution, was maintained thereafter.

All voltammograms were recorded using a multimode polarograph from Princeton Applied Research Model 384B connected with a static mercury drop electrode PAR 303A. A platinum wire was used as an auxiliary electrode and Ag/AgCl (saturated KCl) electrode as a reference.

The measurements were carried out at room temperature.

4. Results and Discussion

4.1. Theoretical Results

The dimensionless voltammetric response of the surface catalytic mechanism is mainly determined by the catalytic parameter γ and the kinetic parameter λ . The catalytic parameter $\gamma = k_c/f$ represents the effect of "catalytic" reaction (II), while the

kinetic parameter $\lambda = k_s/f$ reflects the effect of the charge transfer kinetics on the voltammetric response of the redox reaction (I). The reversibility of the redox reaction is mainly determined by the kinetic parameter λ . The redox reaction appears quasi-reversible if the kinetic parameter is within the interval $-1.5 \leq \log(\lambda) \leq 1$. If $\log(\lambda) > 1$ and $\log(\lambda) < -1.5$, the reaction appears reversible and totally irreversible, respectively.

Figure 1 shows dimensionless voltammograms of a quasi-reversible redox reaction simulated with various catalytic parameter values. It is obvious that the catalytic parameter strongly influences the shape of the forward and the backward components of the SW voltammetric response. Both currents are changed from bell-shaped to the sigmoidal form as the catalytic effect increases. If the catalytic parameter is $\log(\gamma) \geq 0$, the

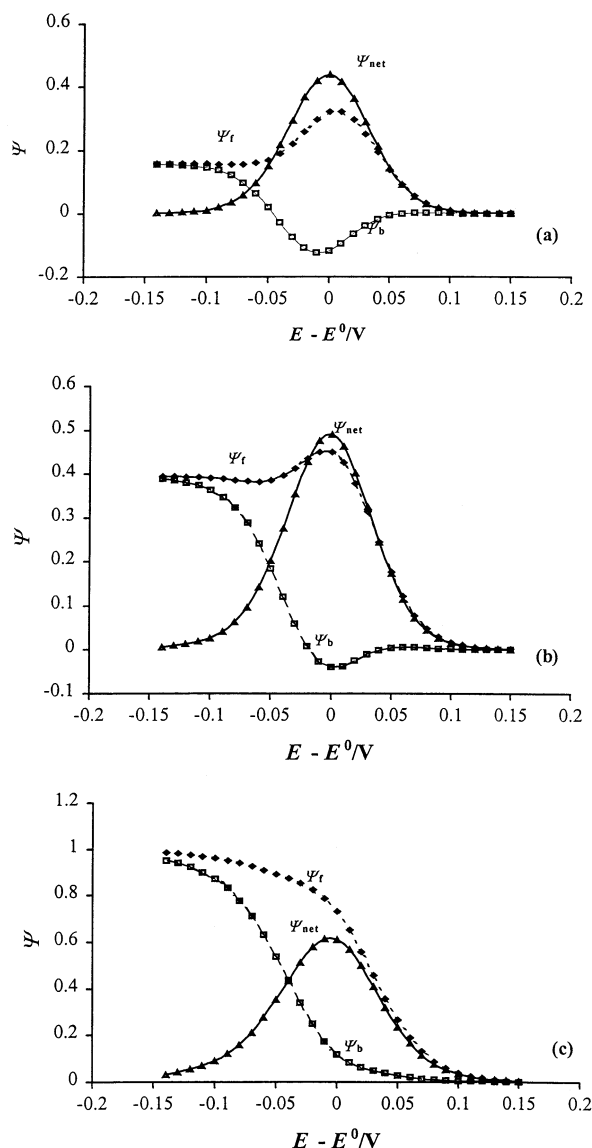


Fig. 1. Effect of the catalytic parameter γ on the dimensionless SWV response of the catalytic surface redox mechanism. The conditions of the simulation are: $\lambda = 2$, nE_{SW} (SW amplitude) = 25 mV, dE (scan increment) = 10 mV, $\alpha = 0.5$. Catalytic parameter is: $\log(\gamma) = -0.8$ (a), -0.4 (b) and 0 (c). Ψ_f , Ψ_b , and Ψ_{net} are the forward, backward and net component of the SWV response, respectively.

backward (reoxidation) component of the SWV response gains the same shape and sign as the forward (reduction) component (see Fig. 1c). Under such conditions, the rate of the catalytic reaction (II) is rapid enough to transform immediately all the amount of the reduced species back to the oxidized form, and the reoxidation process does not occur at all. Interestingly, the radical change in the shape of the forward and backward component exhibits no influence on the shape and position of the net SWV component. For any value of the catalytic parameter, the net-SWV response retains a well-defined bell-shaped form with a readily measurable peak current and peak potential. From an analytical point of view this property can be regarded as an important advantage of the SWV, in comparison with other techniques applied in the study of this mechanism, such for instance, cyclic staircase voltammetry.

The catalytic parameter γ exhibits different influence on both the dimensionless peak currents $\Delta\Psi_p$ and the peak potentials E_p , depending on the reversibility of the redox reaction. In general, regardless the reversibility of the redox reaction, the larger the catalytic parameter, the higher the peak current. Figure 2 represents the relationship between the dimensionless peak currents and the catalytic parameter γ in dependence of the reversibility of the redox reaction. If the redox reaction is close to the reversible region $\log(\lambda) \geq 0.7$, the dimensionless peak currents increase proportional to the catalytic parameter (see curves 1 and 2 in Fig. 2). The higher the reversibility of the redox reaction, the

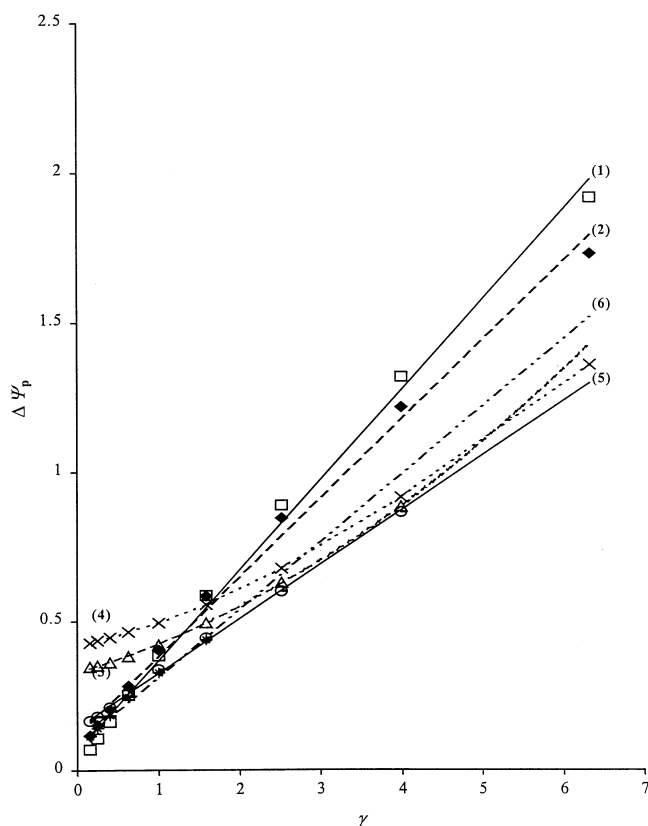


Fig. 2. Dependence of the dimensionless peak currents $\Delta\Psi_p$ on the catalytic parameter γ for varying reversibility of the redox reaction. The conditions of the simulation are: $nE_{sw} = 20$ mV, $dE = 5$ mV, $\alpha = 0.5$ and $\log(\lambda) = 0.90$ (1), 0.67 (2), 0.00 (3), -0.22 (4), -0.70 (5) and -1.00 (6).

larger the slope of the curve representing the $\Delta\Psi_p$ - γ relationship. These results imply that the reversible redox reaction would be the one most sensitive to the rate of the catalytic reaction (II), which means that the reversible surface catalytic mechanism would provide the maximal analytical sensitivity. If the redox reaction was quasireversible, the peak current is a more complex function of the catalytic parameter. The peak currents still enhance with the catalytic parameter, however, the relationship is not linear (see curves 3 and 4 in Fig. 2). It is important to emphasize that the rate of the catalytic reaction exhibits influence on the redox reaction although it appears totally irreversible. As for the reversible redox reaction, the peak current of the totally irreversible redox reaction is a linear function of the catalytic parameter γ , as curves 5 and 6 in Figure 2 illustrate. The latest results are particularly important because it is evident that the catalytic reaction can significantly improve the analytical sensitivity even of a totally irreversible redox reaction.

The influence of the catalytic parameter γ on the potential of the SWV response is depicted in Figure 3. The position of the peak potential of a reversible redox reaction remains virtually insensitive to the increase of the catalytic parameter at a moderate rate of the catalytic reaction ($\log(\gamma) \leq 0.6$) (see curves 1 and 2 in Fig. 3). Within the quasireversible region, the peak potential appreciably shifts towards more negative values with an enhancement of the catalytic parameter (see curves 3 and 4 in Fig. 3). For instance, if $\log(\gamma)$ increases from -0.8 to 0.8 , the peak potential is getting about 130 mV more negative. If the redox reaction is totally irreversible the peak potential linearly shifts in the negative direction with the logarithm of the catalytic parameter with a constant slope of about 75 mV (lines 5 and 6 in Fig. 3).

In addition, the influence of the charge transfer rate, represented through the kinetic parameter λ will be considered. From the theory for the surface redox reaction [11, 12] it is well known that the dimensionless peak current in the SWV depends parabolically on the kinetic parameter λ . The dependence is associated with a sharp maximum located within the quasireversible region. The origin of this phenomenon, called a "quasireversible maximum", is well understood [11–13]. The quasireversible maximum appears to be an essential feature of the entire class of redox reactions in which one or both species of the redox couple are immobilized to the electrode surface. This is an exceptionally important property since it can be utilized for kinetic measurements of the surface redox reaction [13, 14, 18].

The surface catalytic mechanism is also attributed with the quasireversible maximum if the catalytic parameter is within the range $\log(\gamma) \leq 0.3$. A series of quasireversible maxima constructed for a variety of the catalytic parameters, are illustrated in Figure 4. Obviously, the quasireversible maximum is less noticeable with increasing value of the catalytic parameter. When the rate of the catalytic reaction is so rapid to transform the surface reaction into an irreversible redox process ($\log(\gamma) > 0.3$), the quasireversible maximum vanishes. It is important to note that within the interval $-1.5 \leq \log(\gamma) \leq 0.3$, the position of the quasireversible maximum slightly shifts towards higher values of the kinetic parameter λ with the increase of the catalytic parameter γ . Nevertheless, if $\log(\gamma) \leq -1.5$, the position of quasireversible maximum is mainly determined by the charge transfer rate, and hence it can be utilized as a valuable property for estimation of the standard rate constant of the surface catalytic mechanism, according to the procedure which has been developed in the case of a simple surface redox reaction [13, 14, 18]. However, it is worth noting that the latest theoretical analysis cannot be achieved investigating a single redox reaction. The

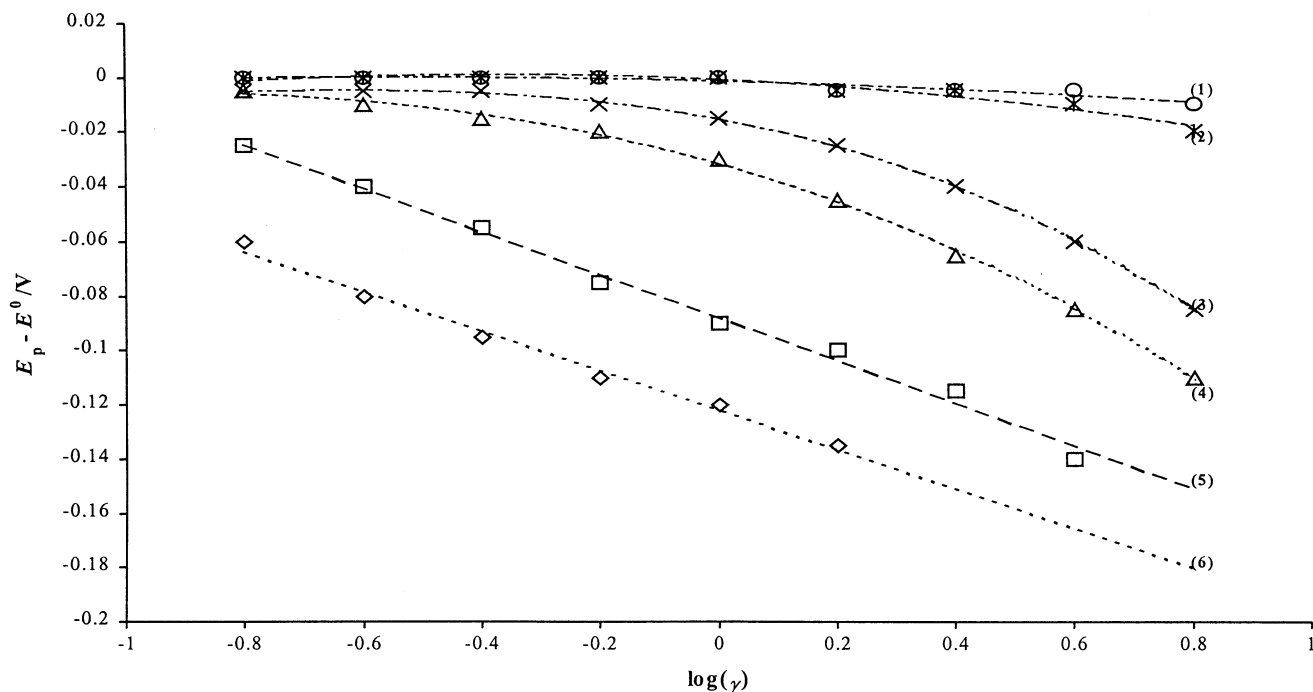


Fig. 3. Dependence of the peak potentials E_p on the catalytic parameter γ for varying reversibility of the redox reaction. The conditions of the simulation are: $nE_{sw} = 20$ mV, $dE = 5$ mV, $\alpha = 0.5$ and $\log(\lambda) = 0.90$ (1), 0.67 (2), 0.00 (3), -0.22 (4), -0.70 (5) and -1.00 (6).

physical meaning of the results presented in Figure 4 corresponds to a comparison of distinct redox reactions of different reversibility, but characterized with the same catalytic parameter.

In the experimental study of a single redox reaction, one can vary the rate of the catalytic regeneration of the reacting substance adjusting the concentration of the catalytic agents. In this way, experimental results corresponding to the theoretical analysis illustrated in the Figures 1–3, could be collected. However, the redox reaction can be also affected by variation of the parameters of the excitement signal such as SW frequency and SW amplitude. The SW frequency exhibits a complex effect on the voltammetric response since it simultaneously influences both the catalytic $\gamma = k_c/f$ and kinetic $\lambda = k_s/f$ parameters. Figure 5 shows simulated results, which corresponds to a real experimental case. During these simulations, the frequency of the signal was altered within a wide interval from 100 to 2000 Hz, keeping all other parameters at a constant value.

Increasing the frequency of the SW signal caused both the catalytic and kinetic parameters to diminish. The decrease of the catalytic parameter results in decreasing of the peak current while the decrease of the kinetic parameter, due to the phenomenon of the quasireversible maximum, exhibits an opposite effect. Which effect will predominate depends on the particular ratio between the catalytic rate constant k_c and the standard rate constant k_s . Approximately, if $k_c/k_s \geq 0.5$, the effect of the catalytic reaction prevails. Under such conditions, the relationship between the peak current and the logarithm of the inverse frequency is characterized with a nonlinear sigmoidal function, without defined maximal value (see curves 1–3 in the Fig. 5). If the ratio $k_c/k_s \leq 0.15$, the electrode reaction is mainly controlled by the charge transfer rate and the relationship $\Delta\Psi_p - \log(f^{-1})$ is associated with the quasireversible maximum which position depends exclusively on the standard rate constant (see curves 5–7 in Fig. 5). Within these boundary values, a complex mixed control of the electrode reaction occurs. In this region, due to the influ-

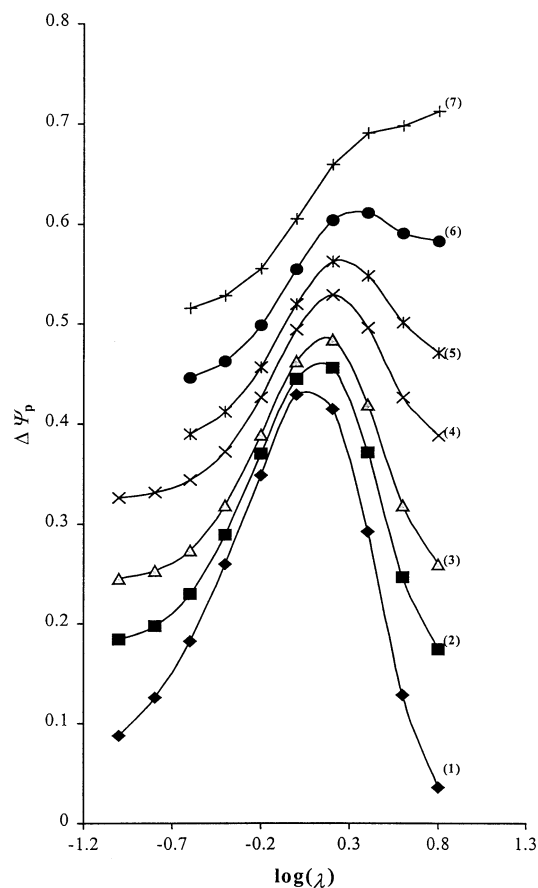


Fig. 4. Effect of the catalytic parameter γ on the quasireversible maximum. The conditions of the simulations are: $nE_{sw} = 20$ mV, $dE = 5$ mV, $\alpha = 0.5$ and $\log(\gamma) = -1.5$ (1), -0.4 (2), -0.2 (3), 0 (4), 0.1 (5), 0.2 (6) and 0.3 (7).

ence of the charge transfer kinetics, the quasireversible maximum appears, however, its position depends on both standard rate constant and the catalytic rate constant.

At the end of this section, an interesting phenomenon under increasing amplitude of the signal will be discussed. Under certain experimental conditions, the single SW peak splits in two peaks symmetrically located around the value of the standard redox potential. The splitting of the net SW peak appears because of a large separation between the forward and backward component of the SW response. This phenomenon was for the first time observed with simple surface redox reaction [12, 15, 18]. Moreover, it was recently demonstrated that the splitting of the peak is an identifiable feature that can be utilized for entire characterization of the simple surface redox reaction. The surface catalytic mechanism is associated with the splitting of the SWV response if the catalytic parameter was $\gamma \leq 2$ (see Fig. 6). The peak at more positive potential slightly diminishes with increasing catalytic parameter, and finally the splitting vanishes if $\gamma > 2$. The potential separation between the split SW peaks does not depend significantly on the catalytic parameter. Therefore, the splitting of the SW response can be used only as a qualitative indicator to recognize the surface catalytic mechanism, however it can not be explored as an identifiable feature for estimation of the catalytic rate constant.

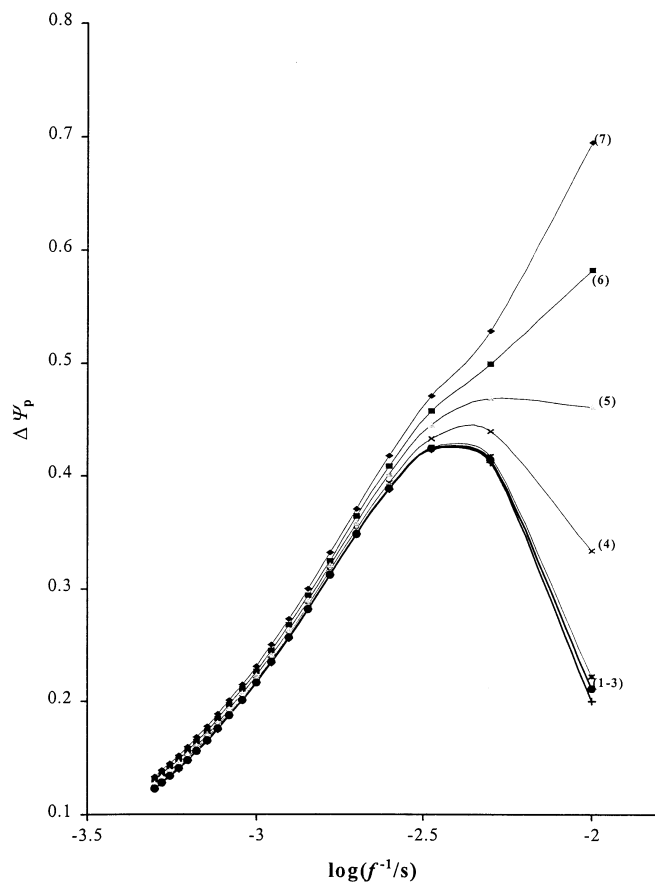


Fig. 5. Dependence of the dimensionless peak currents on the logarithm of the inverse signal frequency for different rates of the catalytic reaction. The conditions of the simulations are: $nE_{sw} = 20$ mV, $dE = 5$ mV, $k_s = 316.23$ s $^{-1}$, $\alpha = 0.5$, and catalytic rate constant $k_c/s^{-1} = 1$ (1), 5 (2), 10 (3), 50 (4), 100 (5), 150 (6), and 200 (7).

Finally, it is important noting that although the splitting of the SW response can serve for qualitative characterization of the surface catalytic mechanism it is a completely undesirable property from an analytical point of view. In the experimental work, which is analytically oriented, one should investigate thoroughly the influence of both SW amplitude and frequency on the voltammetric response in order to select conditions at which the splitting of the SW peak will not appear. In general, on the basis of the theoretical analysis, an amplitude $nE_{sw} \leq 60$ mV is recommended for analytical purposes.

4.2. Experimental Results

The redox reaction of azobenzene at a mercury electrode was frequently explored as a typical experimental model for a surface redox reaction, in which both species of the redox couple are strongly immobilized on the electrode surface [9, 13, 19]. Azobenzene undergoes fast and chemically reversible reduction to hydrazobenzene through two-electron and two-proton redox reaction. In a strong acidic medium, hydrazobenzene irreversibly rearranges to benzidine, and the overall mechanism turns into a surface EC mechanism. In this work, the redox reaction of azobenzene was investigated in the presence of hydrogen peroxide, as an oxidizing agent. Hydrazobenzene, formed by an electrochemical reduction, is reoxidized back to azobenzene by

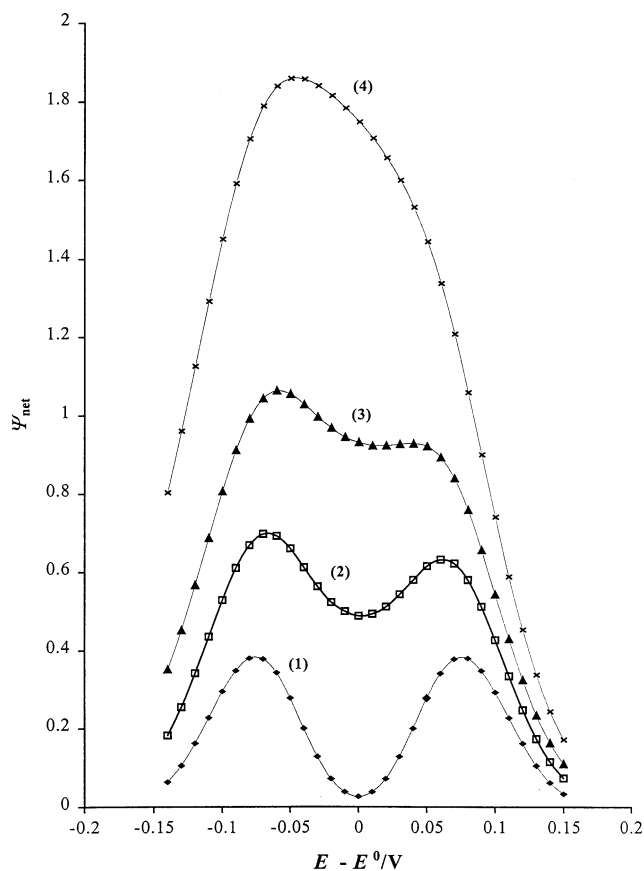


Fig. 6. Effect of the catalytic parameter γ on the split SW response. The conditions of the simulations are: $nE_{sw} = 100$ mV, $dE = 10$ mV, $\alpha = 0.5$, $\lambda = 2$, $\gamma = 0.005$ (1), 0.5 (2), 1 (3), and 2 (4).

means of chemical reaction in the presence of hydrogen peroxide, and the whole electrode reaction turns into a surface catalytic mechanism.

All the experiments were carried out in acetate buffers with a variety of pH. In this medium, the SW voltammetric response of azobenzene, at low amplitudes of the signal, consists of a well-defined single peak. The peak potentials depend on the pH of the medium. The charge transfer rate enhances with an increase of the acidity of the buffers which is in agreement with the literature data [11]. The cyclic voltammograms consist of cathodic and anodic peaks, symmetrically located with respect to the potential

axes. The heights of these peaks are virtually the same, indicating a surface confined redox couple. All these results are in good agreement with the literature data regarding the electrode reaction of azobenzene.

In the acetate buffer of pH 3.2 and SW frequency of $f = 60$ Hz, the redox reaction of azobenzene appears reversible. Adding a certain amount of hydrogen peroxide in the supporting electrolyte, caused the peak current to increase (see Fig. 7) proportional to the amount of hydrogen peroxide, while the peak potentials remain virtually at the same value $E_p = -0.202 \pm 0.002$ V (vs. Ag/AgCl, sat. KCl). These results are in agreement with the

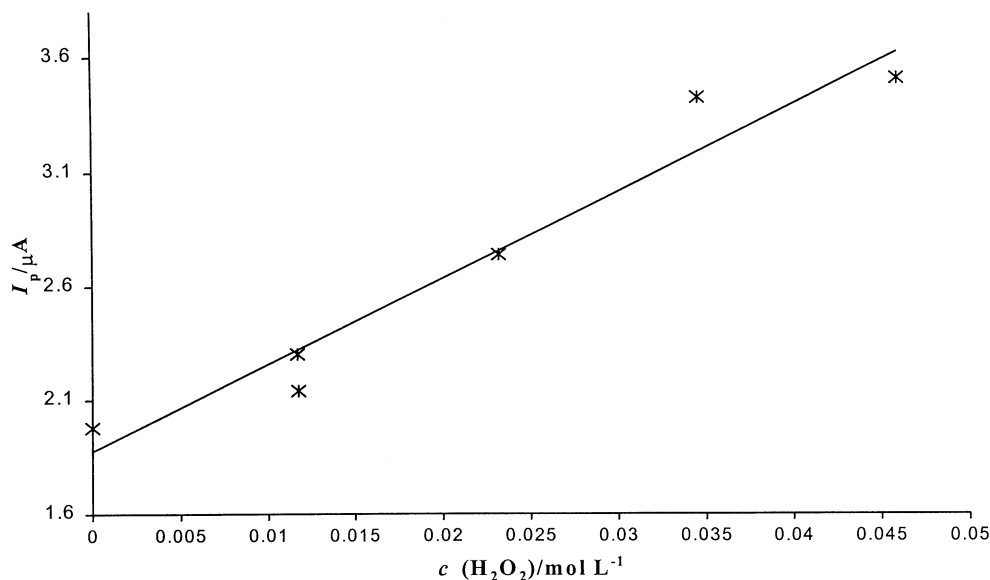


Fig. 7. Influence of hydrogen peroxide on the SW peak currents of 5×10^{-5} mol/L solution of azobenzene recorded in acetate buffer with pH 3.2. The other experimental conditions are: $f = 60$ Hz, $E_{sw} = 20$ mV, $dE = 4$ mV, t_{acc} (accumulation time) = 15 s, E_{acc} (accumulation potential) = 0.0 V.

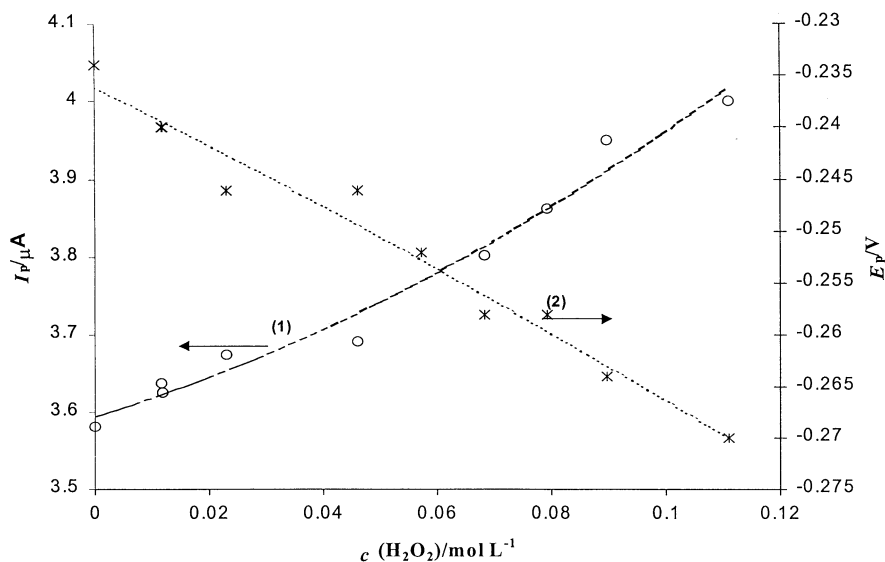


Fig. 8. Influence of hydrogen peroxide on the SWV response of 5×10^{-5} mol/L solution of azobenzene recorded in acetate buffer with pH 4.2. The other experimental conditions are: $f = 40$ Hz, $E_{sw} = 20$ mV, $dE = 4$ mV, $t_{acc} = 15$ s, $E_{acc} = 0.0$ V.

theoretical results obtained for a reversible redox reaction (see curves 1 and 2 in Figs. 2 and 3).

In the acetate buffer with pH 4.2, both peak currents and peak potentials are nonlinear functions of the amount of hydrogen peroxide, presumably due to the quasireversibility of the redox reaction (see Fig. 8). In order to establish this presumption, an attempt was made to estimate the standard rate constant of the redox reaction of azobenzene in this medium in the absence of hydrogen peroxide. In this purpose, the property of the quasireversible maximum was explored. The experimentally measured maximum was compared with the theoretical quasireversible maximum calculated at various values of the standard rate constant k_s . Figure 9 shows a comparison between the theoretically calculated and experimentally obtained quasireversible maximum for azobenzene. The left axes represents the ratio I_p/f , (where I_p is the real peak current and f is the frequency of the signal), which corresponds to the dimensionless peak current $\Delta\psi_p = I_p/(nFS\Gamma_0 f)$ used in the theoretical calculations and shown at the right axes. The theoretical data are calculated under the same instrumental parameters (amplitude of the signal, scan increment and number of electrons $n=2$) such as those used in the experimental measurements. The best fitting between the experimental and the calculated data was observed if the standard rate constant was adjusted at a value of $k_s = 12 \text{ s}^{-1}$. This result confirms the assumption that the redox reaction of azobenzene in acetate buffer with pH 4.2 is quasireversible which explains the nonlinear dependence of the peak currents and the peak potentials on the amount of hydrogen peroxide (see Fig. 8).

Knowing the standard rate constant of the surface redox reaction of azobenzene in acetate buffer with pH 4.2, one could also estimate the catalytic rate constant k_c in the presence of hydrogen peroxide. Figure 10 shows the results collected in this purpose. The left axes shows the differences ΔI_p between the peak current of azobenzene measured in the presence of a certain amount of hydrogen peroxide and the peak current

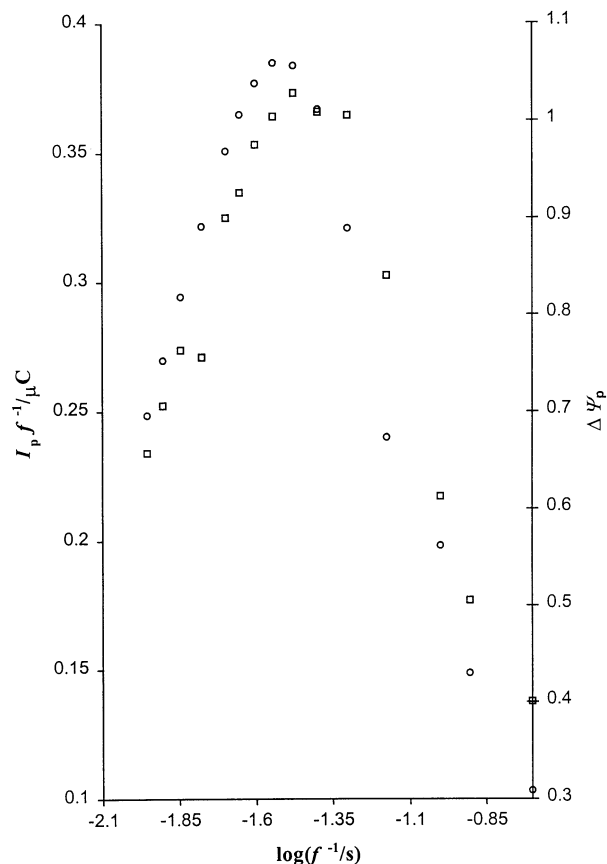


Fig. 9. Fitting of the theoretical (circles, right axes) and the experimental data (squares, left axes) for quasireversible maximum of azobenzene. The experimental conditions are: $c(\text{azo}) = 5 \times 10^{-5} \text{ mol/L}$, pH 4.2 (acetate buffer), $t_{\text{acc}} = 15 \text{ s}$, $E_{\text{sw}} = 50 \text{ mV}$, $dE = 4 \text{ mV}$, $E_{\text{acc}} = 0.0 \text{ V}$. The conditions of the simulations are: $k_s = 12 \text{ s}^{-1}$, $n = 2$, $E_{\text{sw}} = 50 \text{ mV}$, $dE = 4 \text{ mV}$, $\alpha = 0.5$.

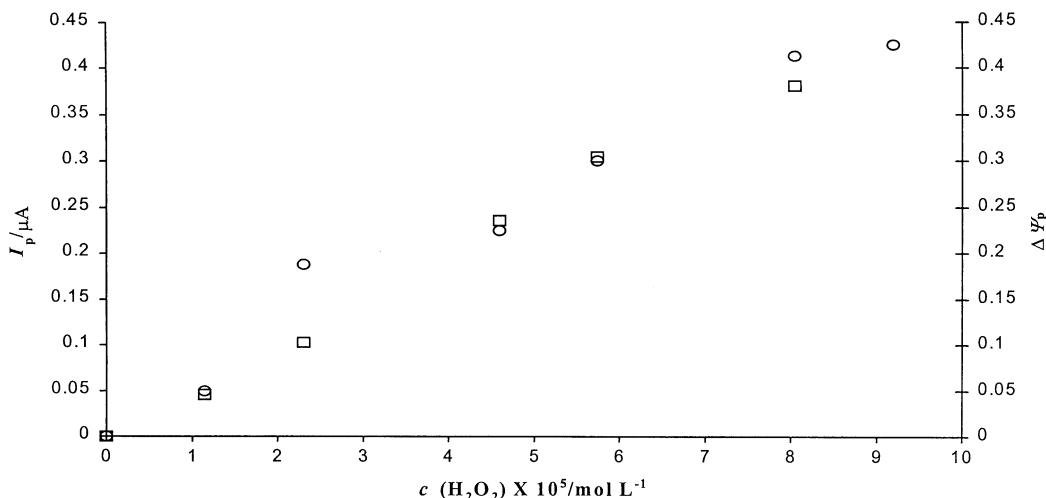


Fig. 10. Influence of hydrogen peroxide on the peak currents of azobenzene (circles) and fitting with the theoretical data (squares) calculated for $k_s = 12 \text{ s}^{-1}$, $k_c = 2.24 \times 10^4 \text{ s}^{-1} \text{ mol}^{-1} \text{ L}$, $\alpha = 0.5$, $n = 2$, $E_{\text{sw}} = 20 \text{ mV}$, $dE = 4 \text{ mV}$. All the experimental conditions are the same as in Figure 8. Left axes represents the differences of the peak currents measured in the presence of a particular amount of hydrogen peroxide and in the absence of it. The right axes represents the differences of the dimensionless peak currents calculated for a surface catalytic mechanism and the simple surface mechanism.

measured in the absence of oxidizing agent ($\Delta I_p = I_p$ (catalytic mechanism) $- I_p$ (simple surface mechanism)). The right axes represents the same differences obtained with numerical simulations which were performed for $k_s = 12 \text{ s}^{-1}$. As can be seen from the Figure 10, the best fitting between the experimental and theoretical data was achieved for catalytic rate constant of $k'_c = 2.24 \times 10^4 \text{ s}^{-1} \text{ mol}^{-1} \text{ L}$. The correlation between the theoretical and experimental data is characterized by a correlation coefficient of $R^2 = 0.9633$. The value of the correlation coefficient can be regarded as a quantitative indicator for the precision of the applied method.

The quasireversible maximum of azobenzene was also measured in the presence of $3 \times 10^{-5} \text{ mol/L}$ hydrogen peroxide in the same acetate buffer. The position of this maximum is in excellent agreement with the position of the theoretical quasireversible maximum calculated for $k_s = 12 \text{ s}^{-1}$ and $k'_c = 2.24 \times 10^4 \text{ s}^{-1} \text{ mol}^{-1} \text{ L}$ (see Fig. 11) which supports the validity of the estimated kinetic constants.

Finally, it should be stressed that the splitting of the SW peak of azobenzene under increasing amplitude of the signal was experimentally observed. The behavior of split SW peaks under influence of increasing concentration of the oxidizing agent is in agreement with the theoretical predictions. The effect of hydrogen peroxide on the split SW peaks is depicted in Figure 12. The SW voltammograms, show that the peak at more positive potential gradually diminishes with increasing rate of the catalytic reaction. The splitting of the SW peak finally vanishes in the presence of 300 mL hydrogen peroxide, which means that under these conditions, the surface reaction of azobenzene is transformed in a totally irreversible redox process. All these experimental results confirm the validity of the presented theory for a surface catalytic redox mechanism.

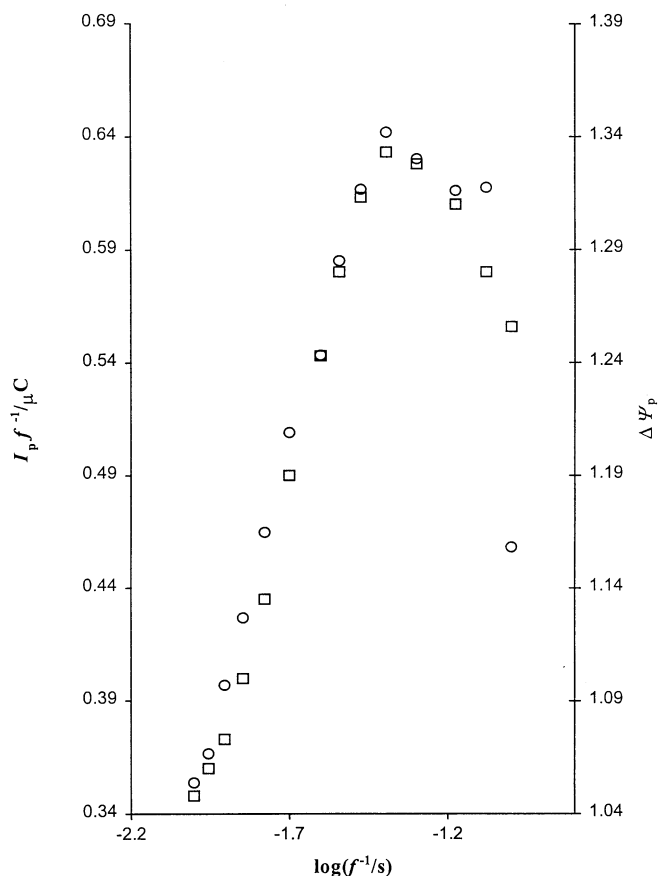


Fig. 11. A comparison of the experimentally measured quasireversible maximum of azobenzene and theoretically calculated quasireversible maximum of a surface catalytic mechanism. The quasireversible maximum of azobenzene was recorded in the presence of $3 \times 10^{-5} \text{ mol/L}$ solution of hydrogen peroxide. Both the experimental and the theoretical conditions are the same as in Figure 9.

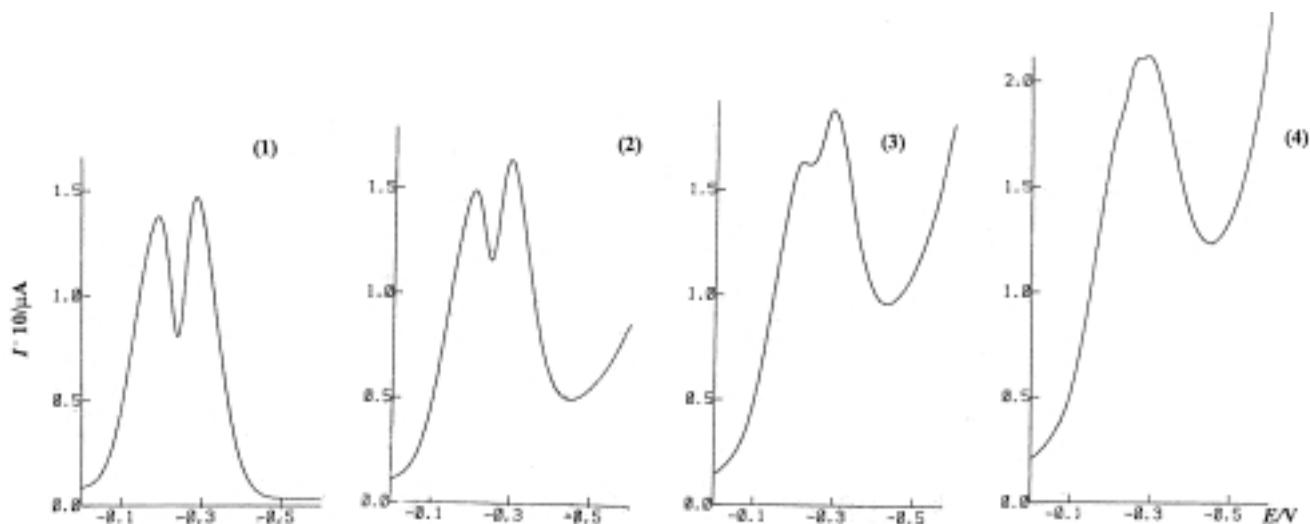


Fig. 12. Influence of hydrogen peroxide on the split SW response of azobenzene. The experimental conditions are: $c(\text{azo}) = 5 \times 10^{-5} \text{ mol/L}$, pH 4.2 (acetate buffer), $t_{\text{acc}} = 15 \text{ s}$, $E_{\text{acc}} = 0.0 \text{ V}$, $E_{\text{sw}} = 150 \text{ mV}$, $f = 40 \text{ Hz}$, $dE = 2 \text{ mV}$ and $c(\text{H}_2\text{O}_2)/\text{mol L}^{-1} = 0$ (1), 0.0116 (2), 0.0231 (3) and 0.0571 (4).

5. References

- [1] R. Brdicka, K. Wiesner, *Collect. Czech. Chem. Commun.* 1947, 12, 39.
- [2] I. Pospisil, *Collect. Czech. Chem. Commun.* 1953, 18, 337.
- [3] S.L. Miller, *J. Am. Chem. Soc.* 1952, 74, 4130.
- [4] P. Delahy, G.L. Stiehl, *J. Am. Chem. Soc.* 1952, 74, 3500.
- [5] R.C. Bess, S.E. Cranston, H.T. Ridgway, *Anal. Chem.* 1976, 48, 1619.
- [6] M.H. Kim, R.L. Birke, *Anal. Chem.* 1983, 55, 522.
- [7] J.J. O'Dea, J. Osteryoung, R.A. Osteryoung, *Anal. Chem.* 1981, 53, 659.
- [8] J. Zeng, R.A. Osteryoung, *Anal. Chem.* 1986, 58, 2766.
- [9] J.J. O'Dea, J.G. Osteryoung, *Anal. Chem.* 1993, 65, 3090.
- [10] J.H. Reeves, S. Song, E.F. Bowden, *Anal. Chem.* 1993, 65, 683.
- [11] Š. Komorsky-Lovrić, M. Lovrić, *J. Electroanal. Chem.* 1995, 384, 115.
- [12] M. Lovrić, Š. Komorsky-Lovrić, *J. Electroanal. Chem.* 1988, 248, 239.
- [13] Š. Komorsky-Lovrić, M. Lovrić, *Anal. Chim. Acta* 1995, 305, 248.
- [14] Š. Komorsky-Lovrić, *Fresenius J. Anal. Chem.* 1996, 356, 306.
- [15] V. Mirčeski, M. Lovrić, *Electroanalysis* 1991, 9, 1283.
- [16] X. Gang, J.J. O' Dea, L.A. Mahoney, J.G. Osteryoung, *Anal. Chem.* 1994, 66, 808.
- [17] R.S. Nicholson, M.L. Olmstead, in *Electrochemistry: Calculations, Simulation and Instrumentation*, Vol. 2 (Eds: J.S. Mattson, H.B. Mark, H.C. MacDonald) Marcel Dekker, New York 1972.
- [18] V. Mirčeski, M. Lovrić, B. Jordanoski, *Electroanalysis* 1999, 11, 660.
- [19] E. Laviron, *J. Electroanal. Chem.* 1973, 42, 415.